Coagulation Factor X-Binding Protein from *Deinagkistrodon acutus* Venom Is a Gla Domain-Binding Protein†

Hideko Atoda,‡ Midori Ishikawa,‡ Hiroshi Mizuno,§ and Takashi Morita*,‡

Department of Biochemistry, Meiji Pharmaceutical University, Noshio, Kiyose, Tokyo 204-8588, Japan, and National Institute of Agrobiological Resources, Tsukuba, Ibaraki 305-8602, Japan

Received May 19, 1998; Revised Manuscript Received August 3, 1998

ABSTRACT: Factor IX/factor X-binding protein (IX/X-bp) is an anticoagulant isolated from the venom of *Trimeresurus flavoviridis* (habu snake) and binds predominantly to factor IX. In this study, we isolated IX/X-bp-like proteins from the venom of *Deinagkistrodon acutus* (hundred pace snake) with binding characteristics different from those of IX/X-bp. The complete amino acid sequence and binding characteristics of the main anticoagulant protein, named X-bp, were investigated. The concentrations of X-bp at half-maximal binding to solid-phase factors X and IX were 0.4 and 3 nM, respectively. The binding of X-bp to solid-phase factor X was inhibited by 50% by 6- and 9-fold excess concentrations of factor X and Gla domain (GD) peptide 1-44, respectively, but was not influenced by GD peptide 1-41 and Gla domainless factor X. X-bp bound two Ca^{2+} ions per molecule with K_d values of 16 ± 0.7 (mean ± SE, $n = 6$) and 103 ± 10 μM. X-bp was a heterodimer of C-type lectin-like subunits. The 16 kDa chain (A chain) consisted of 129 amino acid residues and was 68% identical to the sequence of the A chain of IX/X-bp. The 15 kDa chain (B chain) consisted of 123 amino acid residues and was 87% identical to IX/X-bp. Three-dimensional model construction from the known fold of IX/X-bp showed that amino acid residues different from those of IX/X-bp are mostly on the molecular surface. Some of these are concentrated on a part of the concave surface which is considered to be the coagulation factor-binding site, presumably acting as a discriminator for ligand binding. These results indicated that X-bp isolated from *D. acutus* venom was a GD-binding protein, and the C-terminal region of GD peptide was critical for folding of the peptide.

The anticoagulant proteins IX-bp,[1] factor IX-binding protein, and IX/X-bp (factor IX/factor X-binding protein) from habu snake venom are disulfide-linked heterodimers of C-type lectin-like subunits and bind predominantly to coagulation factor IX in the presence of Ca^{2+} ions (*1*−*3*). The binding sites of IX-bp and IX/X-bp on coagulation factors were localized on the GD region of factors IX and X (*3*, *4*). The crystal structure of IX/X-bp at 2.5 Å resolution demonstrated that a putative binding site of GD is on the concave surface between the two subunits (*5*). Unlike the C-type lectin carbohydrate recognition domain (CRD) fold found in the crystal structure of rat mannose binding protein (MBP) (*6*), a central loop of IX/X-bp projects into the adjoining subunit and contributes to an intertwined dimer in a manner similar to domain swapping. As a result, Ca^{2+} binding sites of IX/X-bp were observed in the helix−loop region different from those of MBP.

While snake venom is known to contain C-type lectins such as *Crotalus atrox* lectin (*7*) and *Lachesis muta stenophyrs* lectin (*8*), homodimers of a Ca^{2+}-dependent carbohydrate recognition domain, many C-type lectin-like heterodimers with various functions have been isolated from Crotalinae and Viperinae snake venom. For example, botrocetin (*9*), bothrojaracin (*10*), jararaca GPIb-bp (*11*), and jararaca IX/X-bp (*12*) were obtained from the venom of *Bothrops jararaca*. These have almost the same molecular mass and show a high degree of structural similarity, but their ligand specificities and biological activities are different from each other.

Snake venoms contain various anticoagulant proteins such as phospholipase A_2, fibrinogenolytic enzymes, protein C-activating enzymes, and proteolytic enzymes that convert coagulation factors into degraded forms (*1*). Many groups have isolated anticoagulant proteins (*1*, *13*−*15*) from the venom of *Deinagkistrodon acutus* without any enzymatic activities mentioned above. It was suggested that some of the *D. acutus* anticoagulant proteins bound to the GD of factor X (*15*, *16*). In this study, we isolated four IX/X-bp-like anticoagulant proteins from *D. acutus* venom with binding characteristics different from those of habu antico-

† This work was partially supported by a Grant-in-Aid for Scientific Research from the Ministry of Education, Science and Culture of Japan and by a Special Grant from the Meiji College of Pharmacy.

* To whom correspondence should be addressed: Department of Biochemistry, Meiji Pharmaceutical University, 2-522-1 Noshio, Kiyose, Tokyo 204-8588, Japan. Telephone: int + 81-424-21-0429 (before August 15) and int + 81-424-95-8479 (after August 18). Fax: int + 81-424-21-0429 (before August 15) and int + 81-424-95-8612 (after August 18).

‡ Meiji Pharmaceutical University.

§ National Institute of Agrobiological Resources.

[1] Abbreviations: IX-bp, factor IX-binding protein; IX/X-bp, factor IX/factor X-binding protein; X-bp, factor X-binding protein; CRD, carbohydrate recognition domain; GD, Gla domain; ECLV, *Echis carinatus leucogaster* venom; ELISA, enzyme-linked immunosorbent assay; HPLC, high-performance liquid chromatography; SDS−PAGE, sodium dodecyl sulfate−polyacrylamide gel electrophoresis.

10.1021/bi981177x CCC: $15.00
Published on Web 11/25/1998

agulants, IX-bp and IX/X-bp. Four anticoagulant proteins bound predominantly to factor X in the presence of Ca^{2+} ions and were named X-bps. The complete amino acid sequence of X-bp 1-1 (hereafter called X-bp) isolated from the main peak was determined, and its binding characteristics were investigated. To obtain further insight into the structure−function relationship, we calculated a molecular model of X-bp using the crystal structure of IX/X-bp. On the basis of the obtained model and comparison with IX/X-bp, the locations not only of the coagulation factor-binding site but also of the region which discriminates between X-bp and IX/X-bp are discussed.

EXPERIMENTAL PROCEDURES

Materials. D. acutus venom was purchased from the Japan Snake Institute (Gunma, Japan). S-Sepharose Fast Flow, Q-Sepharose Fast Flow, Q-Sepharose High Performance, Superdex peptide column, and standard proteins for estimation of molecular mass were obtained from Pharmacia LKB Biotechnology (Uppsala, Sweden). Peroxidase-conjugated goat antibodies against rabbit IgG were purchased from Kirkegaard and Perry Laboratories (Gaithersburg, MD). Finepak SIL $C_{18}S$ and Finepak C_8 columns were obtained from Japan Spectroscopic (Tokyo, Japan). The Cosmosil $5C_{18}$ column was purchased from Nacalai Tesque, Inc. (Kyoto, Japan). All other reagents were of analytical reagent grade or better.

Proteins. Bovine factor X, factor IX, prothrombin, protein C, and protein Z were purified from bovine plasma by the published methods (*17*) with minor modifications. Bovine factor VII was isolated by the method of Saisaka et al. (*18*). Chymotryptic digestion of factor X to prepare derivatives of factor X was performed by the method of Morita and Jackson (*19*), and generated GD peptides and des (1-44) factor X were purified on a Q-Sepharose Fast Flow column. Amino acid compositions of GD peptide 1-41 and of GD peptide 1-44 were confirmed by amino acid analysis.

Isolation of X-bp. All the procedures were performed at 4 °C. Lyophilized *D. acutus* venom was dissolved in 10 mM phosphate buffer (pH 6.8), and a small amount of precipitate was removed by centrifugation for 30 min at 15 000 rpm. The supernatant was applied to a column of S-Sepharose Fast Flow, and the column was washed with the same buffer. Protein was eluted with a linear gradient of 0 to 0.2 M NaCl in 10 mM phosphate buffer (Figure 1a). The anticoagulant activity of eluted fractions was tested by the kaolin-activated PTT assay, and their cross-reactivities with anti-IX/X-bp or anti-X-bp antibodies were tested by ELISA. The kaolin-activated PTT was determined by the method described previously (*1*). IgG against a mixture of X-bp 1-1 and 1-2 was purified from the New Zealand white rabbit serum immunized with the mixture of X-bp 1-1 and 1-2 by affinity chromatography on a column of Protein A-Cellulofine (Seikagaku Kogyo, Tokyo). The ELISA method was described elsewhere (*3*). In this study, we used microtiter plates (Nunc, Roskilde) coated with the eluted fractions, the solution of rabbit IgG against X-bps 1-1 and 1-2 (1 μg/mL), peroxidase-conjugated goat antibodies against rabbit IgG, and the color development solution containing *o*-phenylenediamine (1 mg/mL) and H_2O_2 (0.06%). The absorbance at 492 nm was measured with a microplate reader (MPR-A4, Tosoh, Tokyo, Japan). Materials in peaks 1 and 2 reacted with the antibodies and a prolonged kaolin-activated clotting time. The fractions containing active proteins were pooled and dialyzed against 50 mM Tris-HCl buffer (pH 8.0) and then applied to a column of Q-Sepharose High Performance. After washing with 50 mM Tris-HCl buffer (pH 8.0), proteins were eluted with a linear gradient formed from the starting buffer without NaCl and the same buffer containing 0.2 M NaCl. Purification of peak 1 on the column of Q-Sepharose High Performance is shown in Figure 1b. As shown in Figure 1c, the content in peaks 1-1 and 1-2, designated X-bp 1-1 and X-bp 1-2, respectively, showed similar behavior on SDS−PAGE; both migrated as a 27 kDa band before and 16 and 15 kDa bands after reduction of disulfide bonds. Two proteins analogous to X-bp 1-1 and 1-2, designated X-bp 2-1 and X-bp 2-2, respectively, were obtained from pooled fractions of peak 2, by Q-Sepharose High Performance chromatography (data not shown). X-bps 2-1 and 2-2 exhibited the same behavior on SDS−PAGE as X-bps 1-1 and 1-2 had (Figure 1c).

Binding of X-bp to Coagulation Factors. The binding affinities of X-bp for factor X or other coagulation factors were determined by ELISA as described previously (*3*). Inhibition of the binding of X-bp to solid-phase factor X by GD peptides derived from factor X was demonstrated by the method described previously (*4*).

Dependence of the Binding of X-bp to Factors IX and X on the Concentration of Ca^{2+} Ions. A solution of 50 mM Tris-HCl (pH 8.0) containing 0.1 M NaCl (TBS) was passed over a column of Chelex 100 (Bio-Rad) to remove all traces of calcium. Stock solutions of X-bp, factor IX, and factor X were dialyzed against TBS containing 1 g/L Chelex 100. Factors IX and X were separately fixed on microtiter plates by incubation with solutions of these proteins at 3 nM. After blocking with 1% gelatin, X-bp (0.4 nM for binding to factor X and 2 nM for binding to factor IX) was incubated in the presence of 0−3.2 mM Ca^{2+} ions and 0.1% Tween 20 for 1 h. Each well was washed with TBS containing 0.1% Tween 20 (TBS-TW) and the respective concentration of Ca^{2+} ions, and the bound X-bp was quantified as described elsewhere (*4*).

Equilibrium Dialysis. Equilibrium dialysis was performed at room temperature in a micro dialyzer with 250 μL of cells (Hoffer Scientific Instruments, San Francisco, CA) in 50 mM Tris-HCl and 0.1 M NaCl (pH 8.0). Dialysis membranes were pretreated with a boiled solution of 0.1 M $NaHCO_3$ and 2% EDTA and washed extensively with metal-free water prior to use. The buffers and solutions of proteins used were freed of any possible contamination by metal ions either by passage through a column of Chelex 100 or by dialysis against a suspension of Chelex 100 (1 g/L) in the buffer. A 150 μL aliquot of a solution of $CaCl_2$ containing $^{45}CaCl_2$ as a tracer (100 000 dpm/cell; Dupont, New England Nuclear) was dialyzed against 150 μL of a solution of X-bp (16.5−38 μM, mean of 28.8 μM) for 20 h while the mixture was rotated constantly. Protein-bound Ca^{2+} ions were quantified by liquid scintillation counting.

Electrophoresis. SDS−PAGE was performed by the method of Laemmli (*20*). The molecular mass markers used were phosphorylase b (94 kDa), bovine serum albumin (67 kDa), ovalbumin (43 kDa), carbonic anhydrase (30 kDa),

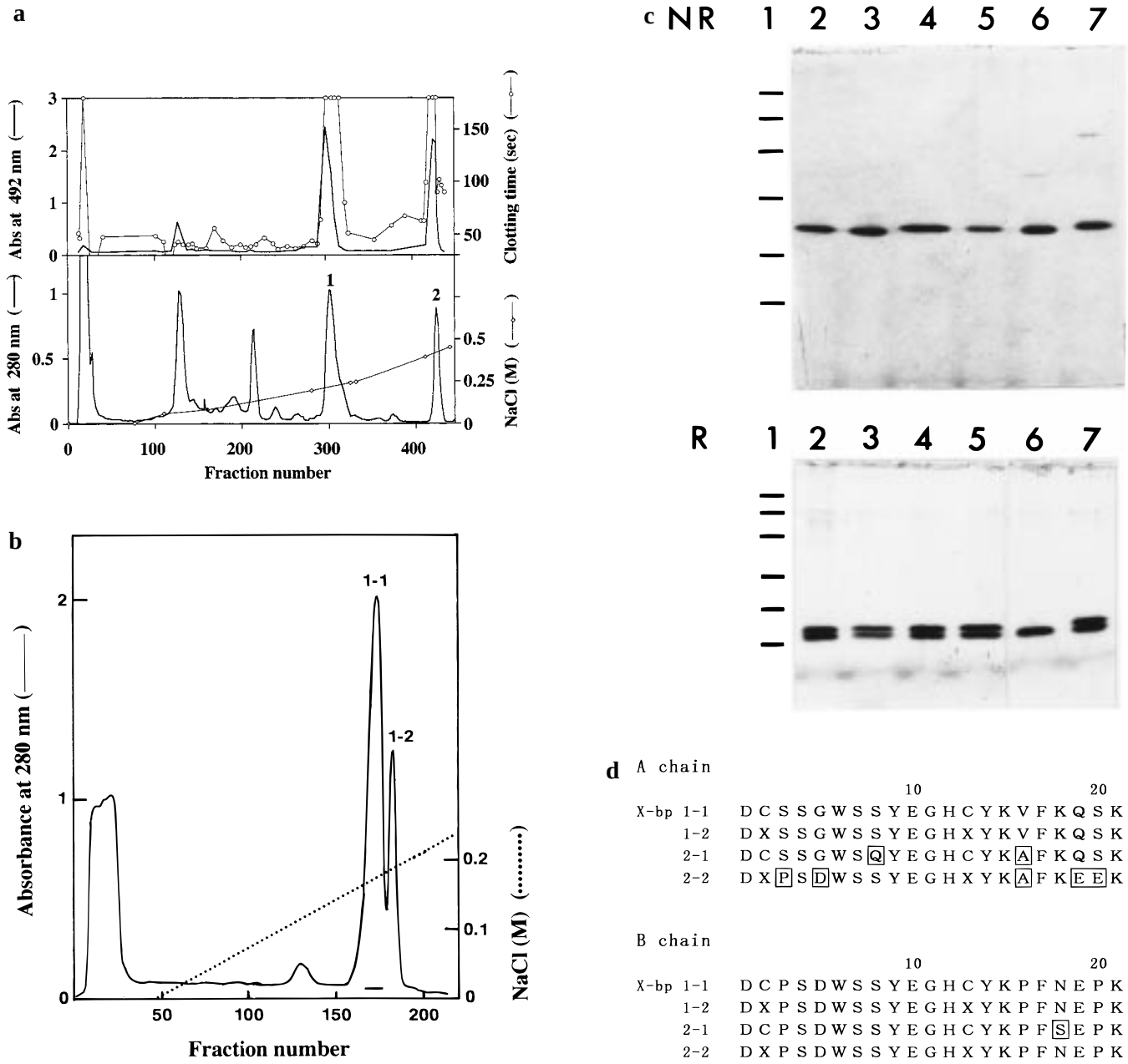

FIGURE 1: Isolation of X-bp. (a) Cation exchange chromatography of *D. acutus* crude venom on an S-Sepharose Fast Flow column. Lyophilized venom (500 mg) from *D. acutus* was applied to a column of S-Sepharose Fast Flow (2.6 cm × 38 cm), and proteins were eluted with linear gradients of 0 to 0.2 M NaCl (750 mL/chamber) and 0.2 to 0.5 M NaCl (500 mL/chamber). Proteins were monitored by absorbance at 280 nm (— in lower panel). The anticoagulant activity in the kaolin-activated PTT assay (○ in upper panel) and reactivity with antibodies against X-bp (−) of the eluted fractions were tested. The cross-reactivity was assayed by ELISA measuring absorbance at 492 nm. Peaks 1 and 2 contained two-chain anticoagulant proteins homologous to IX/X-bp. (b) Anion exchange chromatography of pooled fractions of peak 1 in panel a on a Q-Sepharose HP column. Material in peaks 1-1 and 1-2 reacted with the antibodies against IX/X-bp. Two anticoagulant proteins homologous to IX/X-bp were also isolated from pooled fractions of peak 2 in panel a. (c) SDS−PAGE analysis of the purified proteins under nonreducing (NR) or reducing (R) conditions. Anticoagulant proteins from peak 1-1 (lane 2, X-bp), peak 1-2 (lane 3), peak 2−1 (lane 4), and peak 2-2 (lane 5) were subjected to SDS−PAGE. Lanes 6 and 7 show IX-bp and IX/X-bp, respectively. The molecular mass markers (lane 1) used were phosphorylase b (94 kDa), bovine serum albumin (67 kDa), ovalbumin (43 kDa), carbonic anhydrase (30 kDa), soybean trypsin inhibitor (20.1 kDa), and α-lactalbumin (14 kDa). (d) Amino-terminal amino acid sequence of X-bps. A chain refers to the higher-molecular mass chain, and B chain refers to the lower-molecular mass chain of these proteins. Residues different from those of X-bp 1-1 in each chain are boxed.

soybean trypsin inhibitor (20.1 kDa), and α-lactalbumin (14 kDa).

Amino-Terminal Amino Acid Sequence of X-bps. Reduced and *S*-pyridylethylated X-bps 1-1 and 2-1 or reduced X-bps 1-2 and 2-2 were electrophoresed and electroblotted onto poly(vinylidene difluoride) membranes by following the method of Hirano (*21*). After staining with Amidoblack 10B, the bands were cut out and proteins were analyzed on a gas-phase sequencer.

Determination of the Amino Acid Sequence of X-bp. Purified X-bp was reduced and *S*-pyridylethylated by the methods described elsewhere (*2*). *S*-Pyridylethylated (Pe)-A chain and Pe-B chain were separated by reverse-phase HPLC on a Finepak SIL C_{18}S column. The Pe-A chain was digested

with lysyl endopeptidase (1:50 mole:mole) in 50 mM Tris-HCl buffer (pH 9.5) containing 4 M urea at 34 °C for 17 h, and the peptides generated (AK peptides) were purified by reverse-phase HPLC. The Pe-A chain was also digested with pepsin (1:50 mole:mole) in 0.01 N HCl at 37 °C for 24 h, and the pepsin peptides (AP) were separated by reverse-phase HPLC. Digests of Pe-A chain by chymotrypsin (1:25 mole:mole, AC peptides) and by *Staphysococcus aureus* V8 protease (1:12 mole:mole, AE peptides) were separated on a column of Cosmosil $5C_{18}$. Enzymatic digestion of the Pe-B chain was performed with lysyl endopeptidase (1:100 mole:mole, BK peptides) and chymotrypsin (1:25 mole:mole, BC peptides), and the peptides generated were separated by HPLC with a column of Finepak SIL C_8. The Pe-B chain was cleaved with cyanogen bromide (1:2000 mole:mole), and the fragments, BCN peptides, were separated on a column of Superdex peptide. One of the BCN peptides, BCN1, was subdigested with lysyl endopeptidase (1:100 mole:mole), and the subfragments were separated on a column of Finepak C_8. Amino acid sequences of the purified peptides were determined with a protein sequencer (model 473A, Applied Biosystems, Foster City, CA). Amino acid compositions of peptides were analyzed using an automated amino acid analyzer (model L-8500, Hitachi, Tokyo, Japan) by following the method of Spackman et al. (*22*) after vapor-phase hydrolysis at 110 °C in evacuated, sealed tubes with 5.7 M HCl containing 0.1% phenol for 24 h.

Modeling. The programs QUANTA/PROTEIN and QUANTA/MODELER (Molecular Simulations, Inc.) were used to construct a three-dimensional model of X-bp by adopting its amino acid sequence into the known fold of IX/X-bp. Sequence alignment was not required because of the high degree of homology (68 and 87% sequence identity in A and B chains, respectively) and because there were no gaps in the sequences. The backbone was copied. Side chains were copied where identical, and displaced side chain atom positions were generated in ideal positions from a structure library. QUANTA/CHARMm (Molecular Simulations, Inc.) was used to minimize the obtained model to remove local strain. Further refinement by molecular dynamics or Monte Carlo simulation was not considered necessary.

RESULTS

Amino-Terminal Amino Acid Sequences of the X-bps. Four IX/X-bp-like proteins were obtained from *D. acutus* venom. The amino-terminal amino acid sequences of the X-bps were determined after separation of the two chains by SDS−PAGE of reduced samples and electroblotting onto poly(vinylidene difluoride) membranes (Figure 1d). All four proteins prolonged the kaolin-activated clotting time, and the four anticoagulant proteins showed similar cross-reactivity with anti-X-bp IgG. The yields of X-bps 1-1, 1-2, 2-1, and 2-2 from 1 g of lyophilized crude venom were 20.4, 5.4, 15.0, and 3.4 mg, respectively. In the following studies, we used X-bp 1-1 as X-bp.

Binding Characteristics of X-bp. The properties of binding of the anticoagulant protein X-bp to vitamin K-dependent coagulation factors were investigated by ELISA. As shown in Figure 2, X-bp bound to factor X with a higher affinity than to factor IX. EC_{50} values of X-bp for binding to solid-phase factor X and factor IX were 0.4 and 3.0 nM, respectively. The binding of X-bp (2 nM) to solid-phase factor X was inhibited by 50% in the presence of 11.1 nM liquid-phase factor X, while the concentration causing 50% inhibition of factor IX was 37.3 nM. These data indicated that binding affinity of X-bp for factor X was higher than that for factor IX. X-bp did not bind to solid-phase factor VII, prothrombin, protein Z, or protein C (data not shown). The other three anticoagulant proteins isolated here showed essentially the same binding properties as X-bp (data not shown).

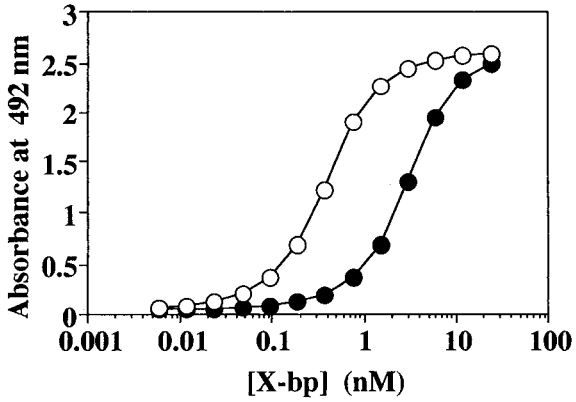

FIGURE 2: Binding of X-bp to solid-phase factors X and IX. X-bp at various concentrations was incubated in the presence of 5 mM Ca^{2+} ions in microtiter wells that had been coated with 18 nM bovine factors X (○) or IX (●). Binding was detected by ELISA with rabbit IgG against X-bp.

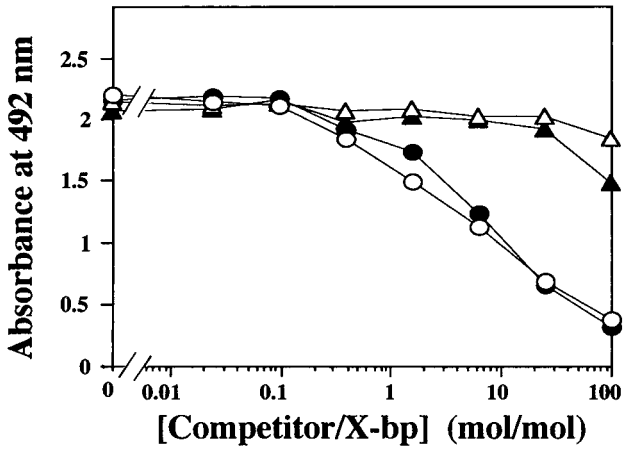

FIGURE 3: Inhibition of binding of X-bp to solid-phase factor X by GD peptide 1-44 but not by GD peptide 1-41. Microtiter wells were coated previously with 9 nM factor X. X-bp (2 nM) and 2 mM Ca^{2+} were incubated in the wells in the presence of various concentrations of factor X (○), GD peptide 1-44 (●), GD peptide 1-41 (▲), or GD-less factor X (△). Bound X-bp was detected by ELISA.

Binding of X-bp to GD Peptide from Factor X. GD peptides 1-44 and 1-41 were prepared by chymotryptic digestion of factor X and the activities of binding of X-bp to these GD peptides were tested. The binding of X-bp (2 nM) to solid-phase factor X was inhibited by 50% by a 6-fold excess of factor X (Figure 3). A 9-fold excess of GD peptide 1-44 also inhibited the binding of X-bp to factor X by 50%, whereas GD peptide 1-41 and Gla domainless factor X did not reduce the extent of binding even when present in 25-fold excess (Figure 3). A 100-fold excess of GD peptide 1-41 reduced the extent of binding by 25%.

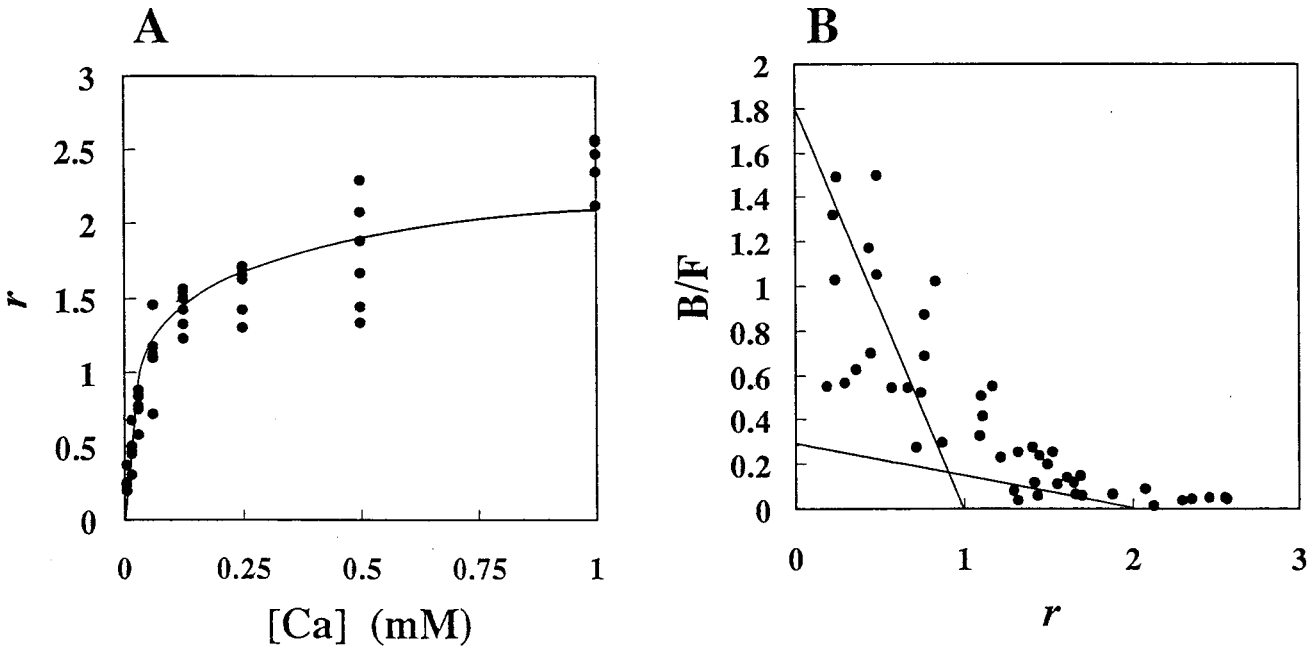

FIGURE 4: Binding of Ca^{2+} ions to X-bp. Binding of Ca^{2+} ions to X-bp was examined by equilibrium dialysis as described in Experimental Procedures. (A) Direct plot of the number of moles of Ca^{2+} bound per mole of protein as a function of the concentration of free Ca^{2+} ions. (B) Scatchard plots of the data shown in panel A. The lines were drawn for the data obtained from six experiments.

Dependence of the Binding of X-bp to Factors X and IX on the Concentration of Ca^{2+} Ions. The binding of X-bp to solid-phase factors X and IX required the presence of Ca^{2+} ions. The dependence on the concentration of Ca^{2+} ions of the extent of binding of X-bp to coagulation factors was investigated using proteins pretreated with Chelex 100 to remove metal ions in the samples. X-bp bound to microtiter plates coated with factor X or factor IX in the presence of 0.2 mM Ca^{2+} ions and reached a plateau at a Ca^{2+} ion concentration of about 1 mM; half-maximal binding to both factors occurred at 0.65 and 0.54 mM Ca^{2+}, respectively. These results were essentially the same as those obtained for IX/X-bp and IX-bp (*3*, *4*).

Ca^{2+} Binding Properties of X-bp. The K_d values of IX-bp were 14 ± 4 and 130 ± 100 μM at pH 7.5 in an isotonic buffer, while those of IX/X-bp were 25 ± 12 and 202 ± 110 μM, respectively (*3*, *23*). In this study, we investigated Ca^{2+} binding to X-bp by equilibrium dialysis at pH 8.0 in an isotonic buffer (Figure 4). X-bp had two independent Ca^{2+}-binding sites with K_d values of 16 ± 0.7 μM (mean $\pm$ SE, $n = 6$) for the high-affinity binding site and 103 ± 10 μM for the low-affinity binding site. These results were essentially the same as those for IX-bp and IX/X-bp.

Complete Amino Acid Sequence of X-bp. X-bp was reduced and *S*-pyridylethylated, and the pyridylethylated (Pe)-A and Pe-B chains were separated by HPLC. Amino-terminal sequencing of the Pe chains identified the first 55 residues of the Pe-A chain and the first 54 residues of the Pe-B chain with the exception of a few residues that could not be identified (Figure 5). Pe-A chain was hydrolyzed with lysyl endopeptidase (AK), pepsin (AP), chymotrypsin (AC), and *S. aureus* V8 protease (AE). Pe-B chain was digested with lysyl endopeptidase (BK) and chymotrypsin (BC). Pe-B chain was also cleaved by CNBr (BCN), and BCN1 peptide was subdigested with lysyl endopeptidase (BCN-K). The fragments were separated by reverse-phase HPLC, and amino acid sequences and compositions of the fragments were analyzed (Table 1). The complete amino acid sequences of the Pe-A and Pe-B chains were determined by arrangement of overlapping peptides as shown in Figure 5. The 16 kDa chain (A chain) consisted of 129 amino acid residues, and the 15 kDa chain (B chain) consisted of 123 amino acid residues.

DISCUSSION

We isolated four X-bps from the venom of *D. acutus*. Analyses of their biological activities and amino-terminal amino acid sequence analysis revealed that these X-bps were structurally and functionally homologous proteins. Isolation of an anticoagulant protein from the venom of hundred pace snake was first reported by Ouyang and Teng (*13*). Sugihara et al. (*14*) isolated two anticoagulant proteins that could correspond to the components in peaks 1 and 2 produced by S-Sepharose Fast Flow column chromatography in this study. Teng and Seegers (*16*) demonstrated that the anticoagulant protein from *D. acutus* venom bound to bovine factor X and activated factor X (factor Xa) and inhibited the conversion of prothrombin to thrombin by the prothrombinase complex. Cox (*15*) also isolated an anticoagulant protein that binds to factor X (Xa) from the venom of *D. acutus* and reported the amino-terminal amino acid sequence of the intact anticoagulant protein which was similar to those of IX/X-bp and X-bps. While amino-terminal amino acid sequences of X-bps determined in this study were very similar with those of the anticoagulant protein reported by Cox, we could not identify which X-bp corresponded to Cox's anticoagulant protein because their sequence was too short. Although Teng and Seegers (*16*) suggested that the binding site of the anticoagulant protein was located in the GD region of factor X, this hypothesis has not been confirmed conclusively. The binding characteristics of X-bp demonstrated in this study indicated clearly that this anticoagulant protein bound to the GD region of factor X (residues 1−44 of the light chain). Vitamin K-dependent coagulation factors bind to the phos-

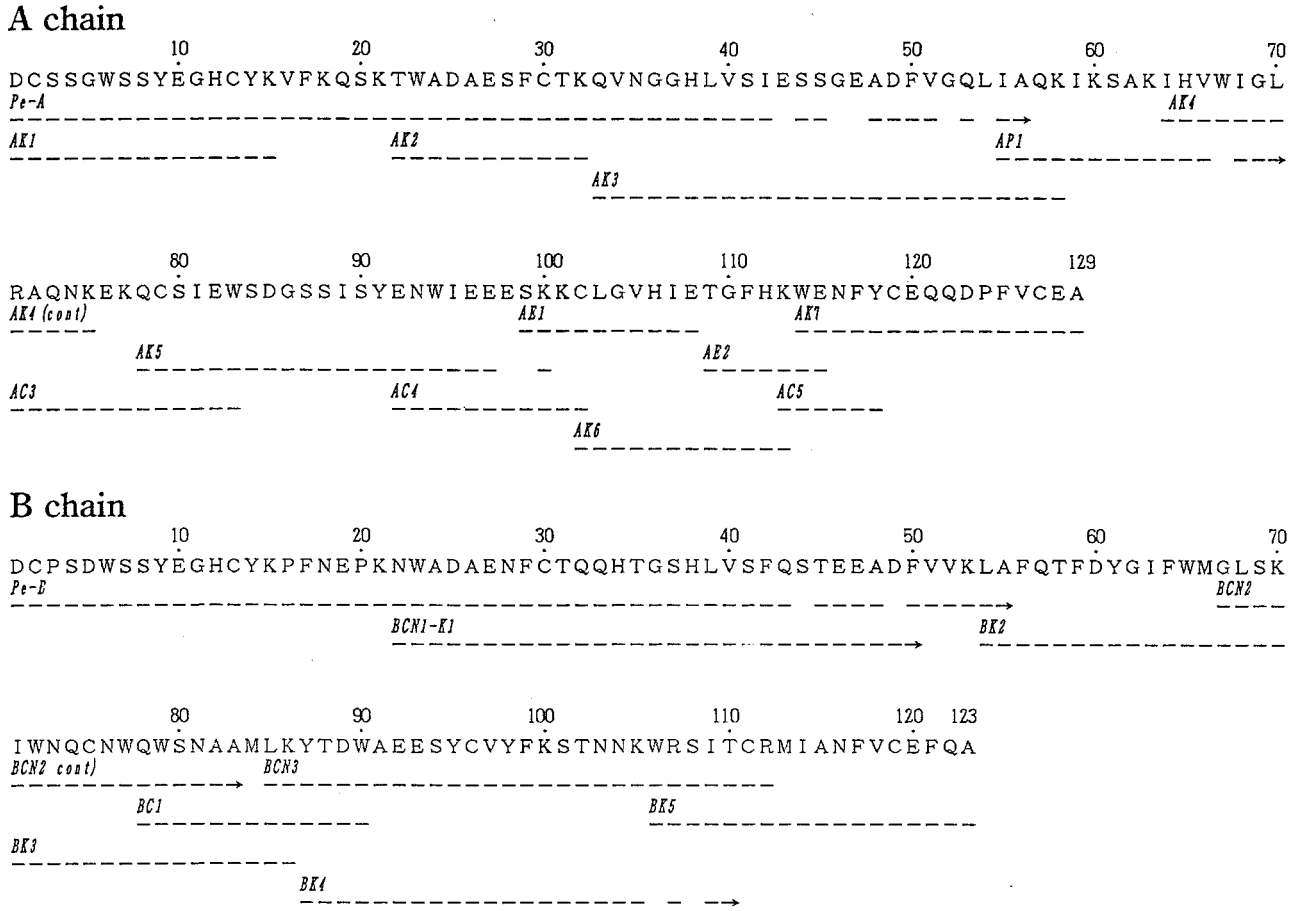

FIGURE 5: Amino acid sequences of the A and B chains of X-bp. Dashes indicate residues identified by sequence analysis of respective peptides. An arrow indicates that the peptide was longer, but that no further residues were identified. Peptides obtained after pyridylethylation (Pe-) and digestion with lysyl endopeptidase (AK and BK), α-chymotrypsin (AC and BC), V8 protease from *S. aureus* (AE), and pepsin (AP), cleavage with CNBr (BCN), and subdigestion with lysyl endopeptidase of BCN1 (BCN1-K1) are shown.

Table 1: Amount Sequenced and Repetitive Yields in the Sequence Analysis of Peptides[a]

peptide	amount sequenced (pmol)	repetitive yield (%)	peptide	amount sequenced (pmol)	repetitive yield (%)
Pe-A	3000	92.9	AE1	nd[b]	89.1
AK1	539	93.6	AE2	nd[b]	84.7
AK2	970	88.6			
AK3	1660	91.8	Pe-B	1048	90.4
AK4	460	87.4	BK2	292	85.6
AK5	241	87.2	BK3	332	89.3
AK6	748	86.6	BK4	293	84.9
AK7	1840	90.2	BK5	250	93.1
AC3	1300	84.1	BCN1-K1	220	89.8
AC4	691	79.8	BCN2	186	81.6
AC5	1068	85.8	BCN3	194	92.5
AP1	nd[b]	92.4	BC1	nd[b]	95.4

[a] Peptides obtained after *S*-pyridylethylation (Pe) and digestion with lysyl endopeptidase (AK and BK), α-chymotrypsin (AC and BC), V8 protease from *S. aureus* (AE), and pepsin (AP), cleavage with CNBr (BCN), and subdigestion with lysyl endopeptidase of BCN1 (BCN1−K1) are used for the sequence analysis. [b] The amino acid composition of the peptide was not determined because of low yield.

pholipid bilayer through their GD region (*24*). Binding of X-bp to the GD region of factor X/Xa should inhibit the formation of the prothrombinase complex on the phospholipid bilayer and reveal anticoagulant activity.

Whereas a 9-fold excess of isolated GD peptide 1-44 and a 6-fold excess of intact factor X inhibited the binding of X-bp to solid-phase factor X by 50%, GD peptide 1-41 showed no such effect even when present in a 25-fold excess. A 100-fold excess concentration of GD peptide 1-41, however, slightly reduced the extent of binding of X-bp to solid-phase factor X. The two GD peptides contained the same number of Gla residues, but the latter lacked three amino acids, Ser-Lys-Tyr, constituting a hinge region between GD- and EGF-domains in the intact factor X molecule (Figure 6). Although the isolated GD peptide had a lower affinity for Ca^{2+} ions, Ca^{2+} ion binding to GD linked to the amino-terminal EGF-like domain was identical to that to intact factor X (*25*). The crystal structure of Ca-prothrombin fragment 1 containing GD reported by Soriano-Garcia et al. (*26*) showed that Phe 41, Trp 42, and Tyr 45 form a cluster of aromatic groups which appears to be critical for folding of the GD by interaction with the disulfide bond of Cys 18−Cys 23 of the conserved disulfide loop as well as with Leu 14, Leu 19, Pro 22, and Leu 32 (see Figure 6). Pollock et al. (*27*) reported that a bovine prothrombin peptide of residues 1−45, but not a peptide of residues 1−42, bound to membranes in a Ca^{2+} concentration-dependent manner. In factor X, the homologous peptide of residues 1−44 bound to membranes in a Ca^{2+} concentration-dependent manner, but the peptide from factor IX containing only residues 1−42 did not bind to membranes (*28*). It was reported that the GD and the adjacent aromatic amino acid stack domain of factor IX (residues 1−47) form the unit responsible for

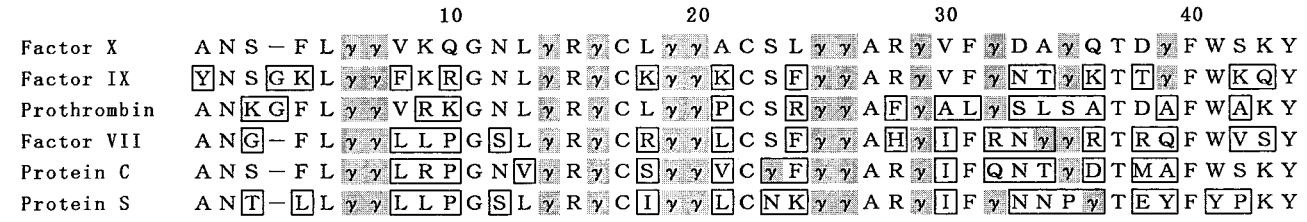

FIGURE 6: Amino acid sequences of GD in various coagulation factors. Amino acid sequences of GD in various bovine coagulation factors are aligned with that of factor X, and different amino acid residues are boxed. Gla residues are marked by γ and shaded.

FIGURE 7: Comparison of the amino acid sequences of IX/X-bp, IX-bp, and X-bp. The sequences of X-bp and IX-bp are aligned with IX/X-bp, and only amino acid residues different from those of IX/X-bp are shown. Residues involved in calcium binding of each chain are shaded. Negatively (▲) and positively (△) charged residues conserved on the putative GD-binding site are marked. Swapped loop-forming residues that contribute to an intertwined dimer are boxed, and the residues of hinge regions are underlined.

binding phospholipid membranes (*29*). The side chains of three amino acids forming the aromatic amino acid stack domain, Phe 41, Trp 42, and Tyr 45, face the interior of the protein near the disulfide loop and stack upon one another. These studies suggested that the aromatic cluster containing Tyr 45 in prothrombin and in factor IX (Tyr 44 in factor X) is essential for folding of the GD needed for interaction with membranes. The GD peptide of factor X which lacks residues 42−44 apparently cannot form the essential fold. While the binding site of X-bp may be localized in the region of GD 1-41, the C-terminal portion of GD peptide 1-44 appears to be necessary to support the correct folding of the GD region and is indispensable for binding to X-bp.

As shown in Figure 7, the 16 kDa chain (A chain) was 73 and 68% identical to the sequences of the A chains of IX-bp and IX/X-bp, respectively, and the 15 kDa chain (B chain) was 87% identical to those of IX-bp and IX/X-bp. Recently, a new factor IX/factor X-binding protein, ECLV IX/X-bp, was isolated from the venom of the Viperinae snake *Echis carinatus leucogaster* (*30*). The α subunit sequence of ECLV IX/X-bp was 56% identical to the A chain of X-bp, and the β subunit of ECLV IX/X-bp was 58% identical to the B chain of X-bp. These observations indicated that the C-type CRD heterodimer homologous to IX/X-bp is distributed throughout not only Crotarinae snakes but also Viperinae snakes and suggested the importance of such proteins for these snakes.

Two other proteins containing IX/X-bp-like structure were isolated from the venom of Viperinae snakes: RVV-X from *Daboia russelli* (*31*, *32*) and carinactivase from *E. carinatus leucogaster* (*33*). These proteins consist of a metalloprotease subunit as a heavy chain and a IX/X-bp-like CRD heterodimer as light chains, and Ca^{2+} ions are required for their activity. RVV-X activates factors IX and X; carinactivase activates prothrombin, and the substrates of these proteins contain GD. It was reported that prothrombin activation by carinactivase is inhibited by the prothrombin fragment 1, GD-containing N-terminal region of prothrombin, and the isolated light chains from carinactivase are capable of binding fragment 1 in the presence of Ca^{2+} ions (*33*). Their light chains might serve as regulator regions that determine the specificity of binding of these snake venom proteases to their respective substrates.

Recently, the crystal structure of IX/X-bp was reported (*5*), and two Ca^{2+}-binding sites were identified. In the A chain, IX/X-bp bound a Ca^{2+} ion through Ser 41, Glu 43, Glu 47, and Glu 128. In the B chain, the Ca^{2+}-binding site consisted of Ser 41, Gln 43, Glu 47, and Glu 120. All these residues were conserved in IX-bp and X-bp. In this study, we showed that X-bp is capable of binding two Ca^{2+} ions per molecule as in the case of IX/X-bp, and the binding affinities of Ca^{2+}-binding sites of X-bp were essentially the same as in the case of IX/X-bp. It was also revealed in this

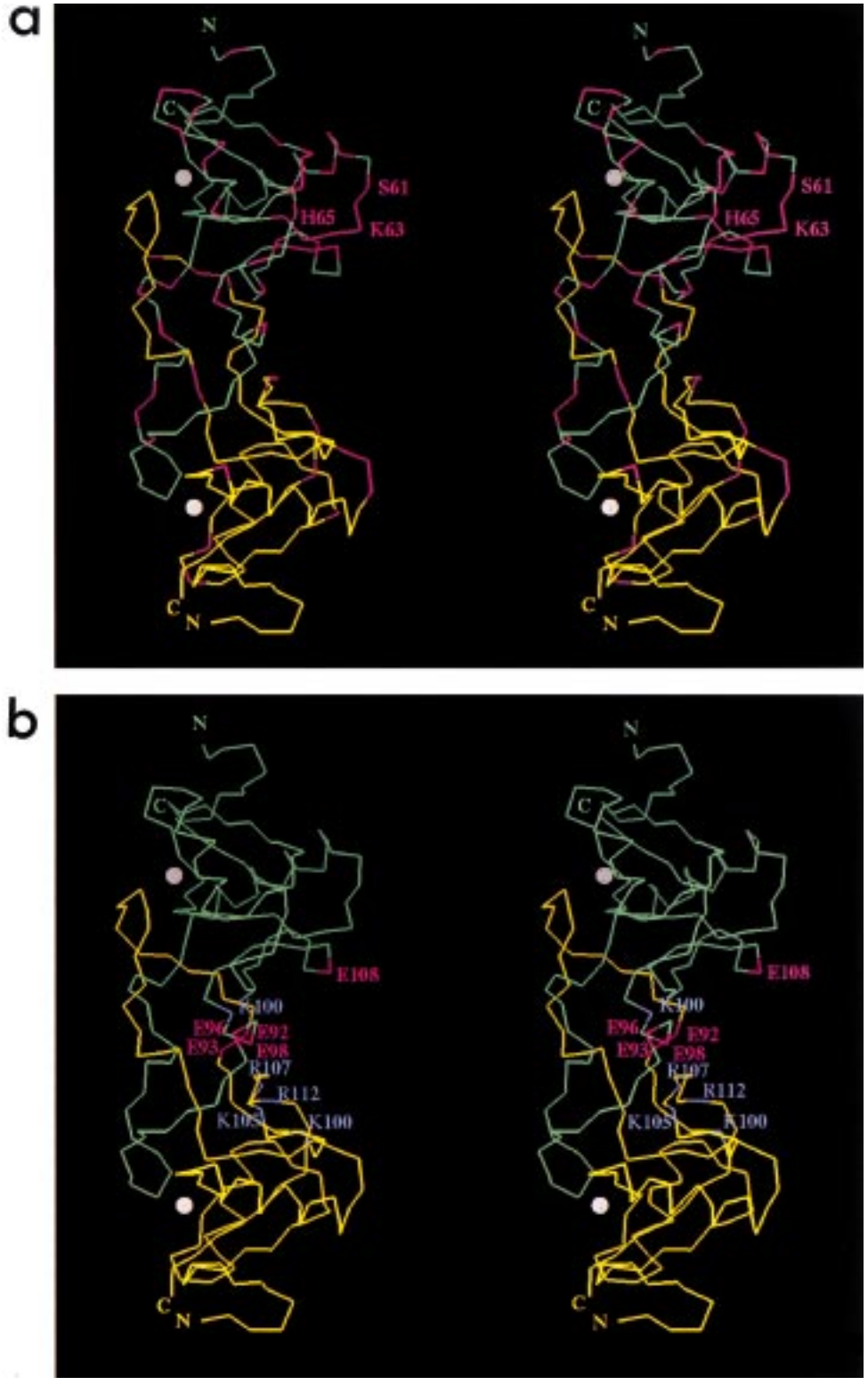

FIGURE 8: Stereoview of the Cα model of X-bp. Subunits A and B are green and yellow, respectively. White spheres indicate Ca^{2+} ions. (a) Amino acid residues differing between X-bp and IX/X-bp are red. Putative discriminator residues are labeled. (b) Conserved basic and acidic residues on the concave surface are blue and red, respectively, and labeled.

study that X-bp binds to GD of factor X. This is essentially the same as for IX/X-bp and IX-bp which bind to GD of their cognate coagulation factors.

The three-dimensional model of X-bp was basically the same as IX/X-bp in the backbone fold. Thus, the most interesting variations were the amino acid sequence differences between the two proteins. Sequences of X-bp and IX/X-bp were aligned without any gaps (Figure 7). Forty residues were different in subunit A, and 16 residues were different in subunit B. The three-dimensional model of X-bp demonstrated that most of these residues are positioned on the molecular surface (Figure 8), and they are usually hydrophilic residues exposed to the solvent. In contrast, most of the hydrophobic residues are buried within the molecule, and are prominently seen in the area surrounded by the C-terminal region of the second α helix, the loop after the

helix, and two β strands in subunit A, where Val 16, Ile 55, Ile 59, Val 66, and Val 105 face each other, forming a hydrophobic core together with residues Val 51, Leu 54, Phe 111, and Val 126 being invariant among X-bp, IX/X-bp, and IX-bp. Concomitant changes of the former five residues might be important for building the precise framework of the main chain, because some residues in this region participate in formation of a part of the concave surface which was suggested to be the GD binding site by the crystal structure of IX/X-bp. Variant residues Ser 61, Lys 63, and His 65 in this site may play a role as discriminators during ligand binding as described later.

The crystal structure of Ca−prothrombin fragment 1 consists of three α helices with seven Ca^{2+} ions bound in an internal cluster between an N-terminal loop and two adjacent helices (*26*). Five Ca^{2+} ions are chelated between Gla 7-Gla 8, Gla 17, Gla 26-Gla 27, and Gla 30 and burried in the GD. The remaining two Ca^{2+} ions are fairly exposed to the solvent, and each is surrounded by only three carboxylate groups of Gla 15 and Gla 20-Gla 21. These Ca^{2+}−ligand clusters possess a partial positive charge, suggesting that they might be utilized in binding interaction with negative charges of phospholipids in the membrane (*34*). Similar binding interactions were considered to occur between X-bp, IX/X-bp, or IX-bp and the cognate GD. In the presence of Ca^{2+} ions, the GD of factor IX and factor X can be accommodated on basically the same fold as prothrombin because of the high degree of sequence homology. Negative carboxylate groups on the concave surface of X-bp, i.e., Glu 96, Glu 98, and Glu 108 in subunit A and Glu 92 and Glu 93 in subunit B, are possibly involved in Gla−Ca^{2+}−Glu interactions because these Glu residues are conserved in X-bp, IX/X-bp, and IX-bp, while Gla residues are highly conserved in GD sequences. On the other hand, positively charged residues Lys 100 in subunit A and Lys 100, Lys 105, Arg 107, and Arg 112 in subunit B which are also conserved and positioned on the concave surface are likely to interact directly with negatively charged Gla residues as suggested by the crystal structure of IX/X-bp. Since 24 oxygen atoms of 16 of 18 carboxylate groups of the nine ordered Gla residues of GD interact with seven Ca^{2+} ions, the remaining oxygen atoms of Gla residues, including disordered Gla 33, are candidates for the salt bridge interaction. This might be the common binding mode between the anticoagulant protein and the cognate GD. Functional differences, for example, X-bp binding mainly to factor X but IX/X-bp binding to factor IX, can be ascribed to amino acid differences on the concave surface generated between subunit A and subunit B. Amino acid residues of subunit B are identical in IX/X-bp and IX-bp so that functional amino acid residues must be in subunit A in this case. The markedly variant amino acid residues are in the vicinity after the second α helix (Figure 8a). Hydrophilic residues 61, 63, and 65 which are exposed to solvent may serve as discriminators for different ligands.

In conclusion, we have determined the complete amino acid sequence of X-bp that binds predominantly to the GD (residues 1−44) of blood coagulation factor X in the presence of Ca^{2+} ions. Our results also indicated that the carboxyl-terminal region of GD peptide 1-44 is critical for the folding of the peptide. The hypothetical binding mode mentioned above should be verified by the X-ray study on the complex formed by X-bp and the GD peptide from factor X. Our investigation should provide new insight into the understanding of the structure and function of the Gla domain in coagulation factor X.

ACKNOWLEDGMENT

We thank Satsuki Hori for performing the amino acid analysis and amino acid sequence analysis and Yoshihisa Suzuki, Junko Iwasaki, Reiko Shimizu, Sachiko Takahashi, Toshiaki Sakuma, Norihiko Ishii, and Yayoi Denda for their assistance with some of the experiments.

REFERENCES

1. Atoda, H., and Morita, T. (1989) *J. Biochem. 106*, 808−813.
2. Atoda, H., Hyuga, M., and Morita, T. (1991) *J. Biol. Chem. 266*, 14903−14911.
3. Atoda, H., Ishikawa, M., Yoshihara, E., Sekiya, F., and Morita, T. (1995) *J. Biochem. 118*, 965−973.
4. Atoda, H., Yoshida, N., Ishikawa, M., and Morita, T. (1994) *Eur. J. Biochem. 224*, 703−708.
5. Mizuno, H., Fujimoto, Z., Koizumi, M., Kano, H., Atoda, H., and Morita, T. (1997) *Nat. Struct. Biol. 4*, 438−441.
6. Weis, W. I., Drickamer, K., and Hendrickson, W. A. (1992) *Nature 360*, 127−134.
7. Hirabayashi, J., Kusunoki, T., and Kasai, K. (1991) *J. Biol. Chem. 266*, 2320−2326.
8. Aragón-Ortiz, F., Reinhard, M., and Auerswald, E. A. (1996) *Toxicon 34*, 763−769.
9. Usami, Y., Fujimura, Y., Suzuki, M., Ozeki, Y., Nishio, K., Fukui, H., and Titani, K. (1993) *Proc. Natl. Acad. Sci. U.S.A. 90*, 928−932.
10. Zingali, R. B., Jandrot-Perrus, M., Guillin, M.-C., and Bon, C. (1993) *Biochemistry 32*, 10794−10802.
11. Kawasaki, T., Fujimura, Y., Usami, Y., Suzuki, M., Miura, S., Sakurai, Y., Makita, K., Taniuchi, Y., Hirano, K., and Titani, K. (1996) *J. Biol. Chem. 271*, 10635−10639.
12. Sekiya, F., Atoda, H., and Morita, T. (1993) *Biochemistry 32*, 6892−6897.
13. Ouyang, C., and Teng, C.-M. (1972) *Biochim. Biophys. Acta 278*, 155−162.
14. Sugihara, H., Nikai, T., Nakamura, T., Daido, H., and Tanaka, T. (1980) *Yakugaku Zasshi 100*, 811−818.
15. Cox, A. C. (1993) *Toxicon 31*, 1445−1457.
16. Teng, C.-M., and Seegers, W. H. (1981) *Thromb. Res. 23*, 255−263.
17. Hashimoto, N., Morita, T., and Iwanaga, S. (1985) *J. Biochem. 97*, 1347−1355.
18. Saisaka, Y., Ueba, J., and Morita, T. (1992) *Nippon Kessen Shiketsu Gakkaishi 3*, 43−48.
19. Morita, T., and Jackson, C. M. (1986) *J. Biol. Chem. 261*, 4015−4023.
20. Laemmli, U. K. (1970) *Nature 227*, 680−685.
21. Hirano, H. (1989) *J. Protein Chem. 8*, 115−130.
22. Spackman, D. H., Stein, W. H., and Moore, S. (1958) *Anal. Chem. 30*, 1190−1206.
23. Sekiya, F., Yamashita, T., and Morita, T. (1995) *Biochemistry 34*, 10043−10047.
24. Furie, B., and Furie, B. C. (1988) *Cell 53*, 505−518.
25. Persson, E., Björk, I., and Stenflo, J. (1991) *J. Biol. Chem. 266*, 2444−2452.
26. Soriano-Garcia, M., Padmanabhan, K., de Vos, A. M., and Tulinsky, A. (1992) *Biochemistry 31*, 2554−2566.
27. Pollock, S. P., Shepard, A. J., Weber, D. J., Olson, D. L., Klapper, D. G., Pedersen, L. G., and Hiskey, R. G. (1988) *J. Biol. Chem. 263*, 14216−14223.

28. Schwalbe, R. A., Ryan, J., Stern, D. M., Kisiel, W., Dahlback, B., and Nelsestuen, G. L. (1989) *J. Biol. Chem. 264*, 20288−20296.
29. Freedman, S. J., Furie, B. C., Furie, B., and Baleja, J. D. (1995) *Biochemistry 34*, 12126−12137.
30. Chen, Y.-L., and Tsai, I.-H. (1996) *Biochemistry 35*, 5264−5271.
31. Takeya, H., Nishida, S., Miyata, T., Kawada, S., Saisaka, Y., Morita, T., and Iwanaga, S. (1992) *J. Biol. Chem. 267*, 14109−14117.
32. Gowda, D. C., Jackson, C. M., Hensley, P., and Davidson, E. A. (1994) *J. Biol. Chem. 269*, 10644−10650.
33. Yamada, D., Sekiya, F., and Morita, T. (1996) *J. Biol. Chem. 271*, 5200−5207.
34. Nelsestuen, G. L. (1984) in *Metal Ions in Biological Systems* (Sigel, H., Ed.) Vol. 17, pp 353−380, Marcel Dekker, Inc., New York.

BI981177X